Journal of Photochemistry and Photobiology A: Chemistry 210 (2010) 1–7

Contents lists available at ScienceDirect

Journal of Photochemistry and Photobiology A: Chemistry

journal homepage: www.elsevier.com/locate/jphotochem

Fluorescence quenching and energy transfer in conjugates of quantum dots with zinc and indium tetraamino phthalocyanines

Jonathan Britton, Edith Antunes, Tebello Nyokong*

Department of Chemistry, Rhodes University, Grahamstown 6140, P.O. Box 94, South Africa

ARTICLE INFO

Article history:
Received 9 October 2009
Received in revised form 9 December 2009
Accepted 15 December 2009
Available online 23 December 2009

Keywords:
Zinc indium tetraaminophthalocyanine
Energy transfer
Fluorescence quenching
Quantum dots

ABSTRACT

CdTe QDs capped with mercapto propionic acid (MPA) and thioglycolic acid (TGA) were covalently linked to zinc and indium tetraaminophthalocyanines (TAPcs) using N-ethyl-N(3-dimethylaminopropyl) carbodiimide (EDC) and N-hydroxy succinimide (NHS) as the coupling agents. The results presented give evidence in favour of formation of an amide bond between the MTAPc and CdTe QDs. Both the linked ZnTAPc–QD complexes and the mixture of QDs and ZnTAPc (without chemical linking) showed Förster resonance energy transfer (FRET), whereas the QD interactions with InTAPc yielded no evidence of FRET. Both MTAPcs quenched the QDs emission, with quenching constants of the order of 10^3–10^4 M^{-1}. High energy transfer efficiencies were obtained in some cases (as high as 93%), due to the low donor to acceptor distances.

1. Introduction

Quantum dots (QDs) are nano-sized semiconductor crystals which exhibit size-dependent physico-chemical properties such as a tunable, narrow emission spectrum, excellent photostability and broad excitation spectra [1–7]. All these properties allow the exploitation of QDs in a variety of fields, including biological labeling, as well as use in photodynamic therapy (PDT) [8] and in nonlinear optics [9].

Metallophthalocyanines (MPcs) are a family of promising photosensitizers for a variety of applications such as in PDT [10–16] and nonlinear optics (NLO) [17,18]. Their distinctive properties such as an intense absorption in the red region of the visible spectrum, effective singlet oxygen generation, coupled with their non-toxicity (in the absence of light) [11–13] have made them a focus of extensive research.

Energy transfer from QDs to different phthalocyanine photosensitizers has been demonstrated in a number of studies [19–22]. The photosensitizer can then accept this energy in a process known as Förster resonance energy transfer (FRET). FRET is a non-radiative energy transfer between the fluorescent donor and a suitable acceptor fluorophore [8]. Apart from the report on the conjugates of SiPc with CdSe QDs through axial ligation [23] and our recent communication on the coordination of a Zn tetraamino phthalocyanine (ZnTAPc) to mercaptopropionic acid (MPA) capped quantum dots [24], the chemical coordination of QDs to the Pc ring has not yet received much attention. In most reported studies, quantum dots were not chemically bound to phthalocyanines. In our recent communication [24], chemically linked QDs showed less FRET than QDs which were physically mixed with ZnTAPc. In order to further explore the conditions required for efficient FRET, in this work we study the FRET between chemically linked ZnTAPc:QDs (capped with TGA) conjugates. The results are compared with those of ZnTAPc:QDs capped with MPA which were reported recently [24]. In addition we report herein on the chemical coordination of a new Pc (ClInTAPc, Fig. 1 inset) with either MPA or TGA capped QDs. With ClInTAPc, a more efficient intersystem crossing to the triplet state is expected compared to ZnTAPc, due to the heavy atom effect. Thus, this work compares the effect of different capping agents, sizes of the quantum dots and central metals in MTAPc complexes on FRET and on quenching of QD emission.

The CdTe QDs (Scheme 1) were chemically linked to the metallo tetraaminophthalocyanines (MTAPc, M = Zn or ClIn, Fig. 1 inset) using linking agents: N-ethyl-N(3-dimethylaminopropyl) carbodiimide (EDC) and N-hydroxy succinimide (NHS), which catalyze the formation of amide bond between the carboxylic acid of QDs and the amine groups of the MTAPc. Jiang et al. [25] have estimated that using this mixture of EDC and NHS, about 60% of carboxylic acid groups are NHS-activated and 30% EDC-activated leaving only 10% unactivated.

2. Experimental

2.1. Materials

N-hydroxysuccinnimide (NHS) was obtained from Fluka. Hydrochloric acid (HCl) and cadmium chloride were

* Corresponding author. Tel.: +27 46 6038260; fax: +27 46 6225109.
E-mail address: t.nyokong@ru.ac.za (T. Nyokong).

1010-6030/$ – see front matter © 2009 Elsevier B.V. All rights reserved.
doi:10.1016/j.jphotochem.2009.12.013

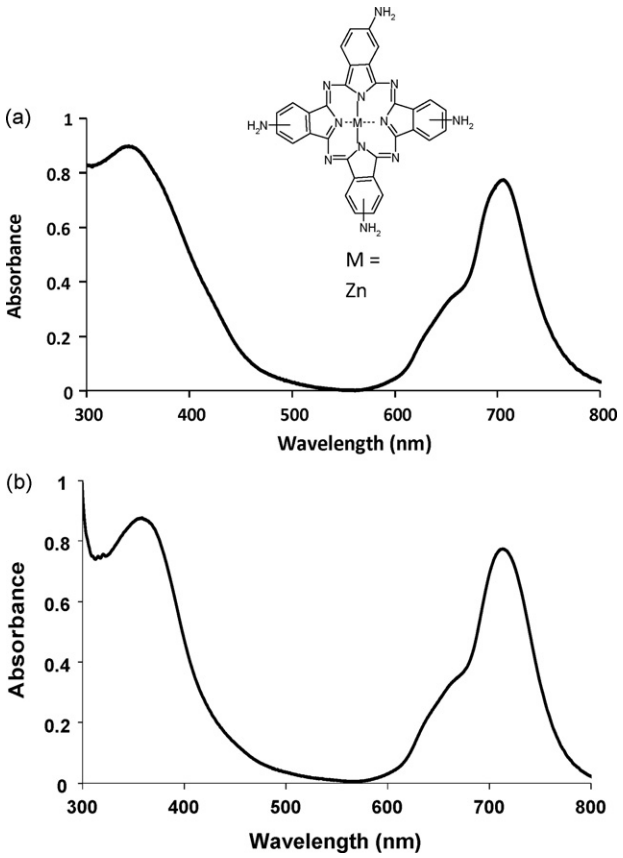

Fig. 1. UV–visible spectrum of (a) ZnTAPc and (b) InTAPc in DMF. Concentration $\sim 1 \times 10^{-6}$ M.

purchased from Merck. Mercaptopropionic acid (MPA), 1,8-diazabicyclo[5.4.0] undec-7-ene (DBU), 1-chloronaphthalene (1-CNP), thioglycolic acid (TGA), tellurium powder, indium chloride and N-(3-dimethylaminopropyl)-N′-ethylcarbodiimide hydrochloride (EDC) were obtained from Sigma–Aldrich. Sodium borohydride, sulphuric acid, dimethylsulfoxide (DMSO), N,N′-dimethylformamide (DMF) and sodium hydroxide pellets were obtained from Saarchem, while urea was purchased from Riedel-de Haën. Zinc tetraaminophthalocyanine (ZnTAPc) was synthesized and characterized according to well established literature methods [26].

2.2. Equipment

Fluorescence excitation and emission spectra were recorded on a Varian Eclipse spectrofluorimeter. UV–visible spectra were recorded on a Varian 500 UV–vis/NIR spectrophotometer. Proton nuclear magnetic resonance (^{1}H NMR) spectra were obtained on a Bruker AMX 400 MHz spectrometer. X-ray powder diffraction (XRD) data was collected with Bruker D8 Discover DCO-B88 EXS009 using a Cu Kα radiation, with a voltage of 30 kV and a current of 40 mA. Samples were run on a silicon crystal sample holder using 6.0 mm slit width at a scan rate of 0.1° 2θ/min.

2.3. Synthesis of indium tetraaminophthalocyanine (ClInTAPc)

ClInTAPc was synthesized according to methods reported for other MTAPc [26] complexes as follows: indium chloride (0.04 g, 0.18 mmol), 4-aminophthalonitrile (0.1 g, 0.7 mmol) and DBU (0.1 ml) in 1-chloronaphthalene (10 ml) were heated under reflux at 220 °C for 7 h. The product was then washed (using Soxhlet apparatus) with methanol, an HCl solution and acetone to remove impurities and starting materials.

Yield: 0.0221 g, 17%. UV–vis (DMF): λ_{max} nm (log ε) 374 (4.54), 711 (4.56), IR: KBr pellets (cm^{-1}): 3453.18 (N–H str.), 3129.17, 3059.56, 3025.36, 2852.14, 2533.11, 2361.17, 2343.29, 2230.38, 1770.24, 1722.41, 1657.80 (C=C str.), 1609.11 (N–H bend), 1525.21, 1481.31, 1435.21, 1386.15, 1335.74 (C–C str.), 1253.12 (C–C str.), 1140.36 (C–C str.), 1041.28 (C–N str.), 928.11, 905.15, 846.43, 745.61, 724.68, 697.34, 661.16, 523.59, 478.65. ^{1}H NMR (DMSO-d_6): δ = 8.30 (4H, s, Ar-H), 8.18 (d, 4H, Ar-H), 8.03 (4H, d, Ar-H). Calcd for $C_{32}H_{20}N_{12}ClIn$: C, 53.17; H, 2.76; N, 23.26%. Found: C, 52.81; H, 3.42; N, 22.88%.

2.4. Synthesis of CdTe QDs capped with mercapto propionic acid (MPA) or thioglycolic acid (TGA)

The preparation of an MPA or TGA capped QD was performed via a modified method adopted from literature [20,27]. Briefly, 2.35 mmol of $CdCl_2 \cdot H_2O$ was dissolved in 125 ml of water and 5.7 mmol of the MPA or TGA stabilizer was added under stirring. The solution was adjusted to pH 11 by the dropwise addition of NaOH. Nitrogen gas was bubbled through the solution for about 1 h, and this aqueous solution subsequently reacted with H_2Te gas. H_2Te gas was generated by the reaction of $NaBH_4$ with Te powder in the presence of 0.5 M H_2SO_4 under a flow of nitrogen gas. The solution was then refluxed under air at 100 °C for different times to control the size of the CdTe QDs. On cooling, the QDs were precipitated out of the solution using excess ethanol; the solutions were then centrifuged to harvest the QDs.

The size of the quantum dots were estimated using the polynomial fitting function derived in the literature [28], Eq. (1):

$$D = (9.8127 \times 10^{-7})\lambda^3 - (1.7147 \times 10^{-3})\lambda^2 + (1.0064)\lambda - (194.84) \quad (1)$$

where λ is the absorption maxima of the QDs. The sizes of the QDs ranged from 2.7 to 4.0 nm (using Eq. (1)). The size was also confirmed using XRD and the Scherrer Eq. (2):

$$d(\text{Å}) = \frac{k\lambda}{\beta \cos\theta} \quad (2)$$

where k is an empirical constant equal to 0.9, λ is the wavelength of the X-ray source, (1.5405 Å for Cu), β is the full width at half maximum of the diffraction peak, and θ is the angular position of the peak. The sizes determined by the two methods were found to be comparable. For FRET studies CdTe–TGA QDs of ~3 nm size and CdTe–MPA QDs of ~3.5 and ~3.0 nm sizes were employed.

For the formation of the amide linked QD–MTAPc, the mixture containing 2 mM NHS, 5 mM EDC, CdTe QDs (0.11 g/ml) and MTAPc (3.8×10^{-5} M) in pH 7.4 buffer was allowed to react for 1 h. NHS

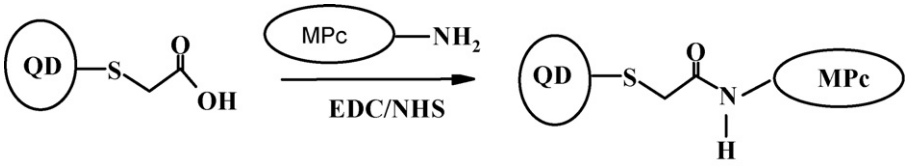

Scheme 1. Linking of QD to MTAPc using EDC/NHS as coupling agents. MPc–ZnTAPc, InTAPc and QD represents CdTe QDs.

and EDC were used for the activation of the carboxylic acid group of the QDs, and the resulting complex is represented as linked QD–MTAPc. Experiments, where the MTAPc were mixed with QDs, without chemical linking, resulting in mixed QD–MTAPc were also performed.

2.5. Fluorescence studies

Fluorescence quantum yields (Φ_F) were determined by a comparative method [29] using Eq. (3):

$$\Phi_F = \Phi_{F(\mathrm{Std})} \frac{F \cdot A_{\mathrm{Std}} \cdot n^2}{F_{\mathrm{Std}} \cdot A \cdot n_{\mathrm{Std}}^2} \quad (3)$$

where F and F_{Std} are the areas under the fluorescence curves of the MTAPc derivatives and the reference, respectively. A and A_{Std} are the absorbances of the sample and reference at the excitation wavelength, and n and n_{Std} are the refractive indices of solvents used for the sample and standard, respectively. ZnPc in DMSO was used as a standard, $\Phi_F = 0.20$ [30], for the determination of the fluorescence quantum yields of the ZnPc derivatives in a 3:2 DMF:water solvent mixture. Rhodamine 6G in ethanol (with $\Phi_F = 0.94$) was employed as the standard for the determination of the fluorescence quantum yields of quantum dots [31,32]. The sample and the standard were both excited at the same relevant wavelength. The fluorescence quantum yields of the QDs are represented as $\Phi_{F(\mathrm{QD})}$, where QD represents TGA or MPA capped CdTe QDs, while for the MTAPc complexes, the Φ_F are represented as $\Phi_{F(\mathrm{MTAPc})}$. The determined fluorescence quantum yield values of the QDs were employed in determining their fluorescence quantum yields in the mixture with MTAPc derivatives ($\Phi_{F(\mathrm{QD})}^{\mathrm{Mix}}$) or $\Phi_{F(\mathrm{QD})}^{\mathrm{linked}}$ linked using Eq. (4):

$$\Phi_{F(\mathrm{QD})}^{\mathrm{Mix}} = \Phi_{F(\mathrm{QD})} \frac{F_{\mathrm{QD}}^{\mathrm{Mix}}}{F_{\mathrm{QD}}} \quad (4)$$

where $\Phi_{F(\mathrm{QD})}$ is the fluorescence quantum yield of the QDs alone and was used as standard, $F_{\mathrm{QD}}^{\mathrm{Mix}}$ is the fluorescence intensity of QDs (in the mixture with, or linked to, the MTAPc) when excited at the excitation wavelength of the QDs (550 nm) and F_{QD} is the fluorescence intensity of the QD alone at the same excitation wavelength.

Fluorescence quenching studies were performed to determine the quenching ability of MTAPc on QDs using a mixture of the two solutions. For the quenching studies of QDs fluorescence by MTAPc, a solution of the 3.0 nm sized QD–TGA was titrated with varying concentrations ($0–1.2 \times 10^{-4}$ M) of the MTAPc derivatives in DMF:water (3:2). These mixtures represent mixed QD:MTAPc, and the solvent mixture employed was used in order to enable both MTAPc and the QDs to dissolve. In monitoring the QDs emission, the excitation wavelength used was at 550 nm and emission spectrum recorded between 560 and 800 nm. The steady decrease in the fluorescence intensity of QDs with an increase in the concentration of MTAPc complexes was related to MTAPc concentrations by Eq. (5) [33]:

$$\frac{F_0}{F} = 1 + K[\mathrm{MTAPc}] \quad (5)$$

where K represents the quenching constant, F_0 and F are the fluorescence intensities of the QDs in the absence and presence of MTAPc (M = Zn or ClIn) respectively.

The number of binding sites on the QDs was determined for the mixed QD–MTAPc using Eq. (6):

$$\log\left[\frac{F_0 - F}{F - F_\infty}\right] = \log k_{\mathrm{b}} + n \log[\mathrm{MTAPc}] \quad (6)$$

where F_0 and F are the fluorescence intensities of QDs in the absence and presence of MTAPc (M = Zn or ClIn), respectively; F_∞, the fluorescence intensity of QDs saturated with MTAPc; k_{b}, the binding constant; n, the number of binding sites on a QD. Plots of $\log\left[\frac{F_0-F}{F-F_\infty}\right]$ against log [MTAPc] provided the values for n (from slope) and k_{b} (as determined from the intercept).

2.6. Determination of FRET parameters

FRET is highly dependent on the following parameters: the center-to-center separation distance between donor and acceptor (r), the degree of spectral overlap of the donor's fluorescence emission spectrum and the acceptor's absorption spectrum (J) [32,34]. FRET efficiency (*Eff*) is determined experimentally from the fluorescence quantum yields of the donor in the absence ($\Phi_{F(\mathrm{QD})}$) and presence ($\Phi_{F(\mathrm{QD})}^{\mathrm{Mix}}$ or $\Phi_{F(\mathrm{QD})}^{\mathrm{linked}}$) of the acceptor using Eq. (7) [32,34]:

$$Eff = 1 - \frac{\Phi_{F(\mathrm{QD})}^{\mathrm{Mix}}}{\Phi_{F(\mathrm{QD})}} \quad (7)$$

FRET efficiency (*Eff*) is related to r (Å) by Eq. (8) [32]:

$$Eff = \frac{R_0^6}{R_0^6 + r^6} \quad (8)$$

where R_0 (the Förster distance, Å) is the critical distance between the donor and the acceptor molecules at which the efficiency of energy transfer is 50% and depends on the quantum yield of the donor, Eq. (9) [32]:

$$R_0^6 = 8.8 \times 10^{23}\, \kappa^2\, n^{-4}\, \Phi_{F(\mathrm{QD})} J \quad (9)$$

where κ^2 is the dipole orientation factor; n, the refractive index of the medium; Φ_{F}, the fluorescence quantum yield of the donor in the absence of the acceptor; and J is the Förster overlap integral, defined by Eq. (10):

$$J = \int f_{\mathrm{QD}}(\lambda)\varepsilon_{\mathrm{MTAPc}}(\lambda)\lambda^4 \partial\lambda \quad (10)$$

where f_{QD} is the normalized QD emission spectrum; and $\varepsilon_{\mathrm{MTAPc}}$, the molar extinction coefficient of MTAPc complexes. In this case, it is assumed that κ^2 is 2/3; such assumptions are often made for donor–acceptor pairs in a liquid medium, since their dipole moments are considered to be isotropically oriented during the excited state lifetimes. λ is the wavelength of the acceptor, which is the Q band. FRET parameters were computed using the program PhotochemCAD [35].

3. Results and discussion

3.1. Absorbance and fluorescence spectra

Fig. 1(a) shows the UV–vis spectrum of ZnTAPc, which is typical of amino phthalocyanine complexes, with a Q band at 702 nm in DMF. The red-shift in the spectrum compared to unsubstituted ZnPc (670 nm) is as a result of the electron-donating ability of the amino groups. Fig. 1(b) is the UV–vis spectrum of InTAPc with a Q band at 713 nm in DMF. The InTAPc complex is more red shifted as expected than ZnTAPc, due to the electronic effects of the large central metal.

QDs grow through the Ostwald ripening process during the course of heating. As they grow, both the absorbance and the emission spectra shift to longer wavelengths. The MPA capped CdTe QDs displayed their first emission peak at 512 nm after 30 min of refluxing and were grown until their emission peak reached a maximum of 746 nm indicating different sizes, Fig. 2. The TGA capped CdTe were grown to ~3 nm in size.

The X-ray diffraction pattern of the MPA capped CdTe QDs employed in this work is shown in Fig. 3. The diffraction pattern shows the three characteristic peaks expected for bulk CdTe structure. Sizes, using XRD (Fig. 3), were found to range between 2.98 and

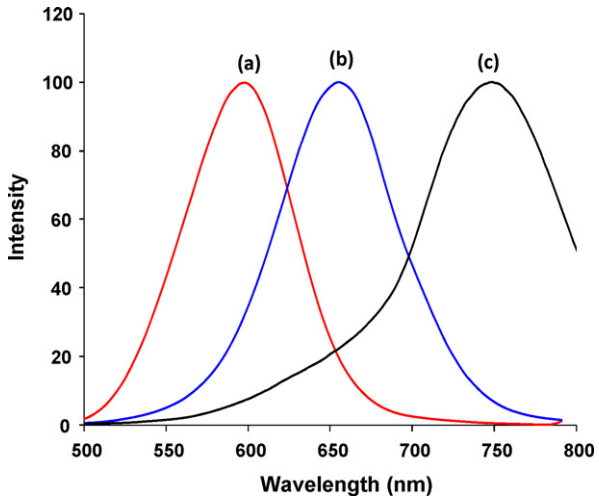

Fig. 2. Emission spectra of different sizes of MPA QDs (a) 3.0 nm, (b) 3.5 nm and (c) 4.1 nm. pH 11 buffer. Excitation = 400 nm.

3.35 nm, and are therefore in the same range as those determined by the polynomial (2.7–4.0 nm).

Fig. 4 overlays the absorption and emission spectra of the CdTe–MPA QDs. The absorption spectra are broad, whereas the emission spectra display narrow well-defined peaks with a full width at half maximum (FWHM) around 60 nm, typical of QDs [5].

CdTe QDs were mixed with MTAPc, (in the absence of EDC/NHS) represented as mixed QD:ZnTAPc, as well as linked with MTAPc using ECD/NHS (represented as linked QD–ZnTAPc). For the mixed QD:ZnTAPc, the mode of interaction is thought to be most likely due to adsorption. The UV/visible spectra (Fig. 5) showed that there is only a 2 nm shift of the Q band from 706 nm (for ZnTAPc alone or mixed QD–ZnTAPc in DMF:water) to 704 nm for linked QD–ZnTAPc.

With the linked QD–MTAPc, the capping agent located on the surface of CdTe QDs were linked to MTAPc by coupling the carboxylic group of the capping agent to the amine group on MTAPc. EDC/NHS mixture was used to activate the carboxylic acid group of the capping agent on the QDs to facilitate this linkage with the amine group of MTAPc, Scheme 1. However, it is possible for more than one amino group of the MTAPc to be linked to the QDs. The linked QDs–ZnTAPc complex was purified and separated from unlinked QDs or ZnTAPc by precipitating it out with THF and ethanol, which were afterwards evaporated off. This was followed by rinsing and centrifuging the solids with water, then acetone to remove the unlinked QDs, thus ensuring that the effects of

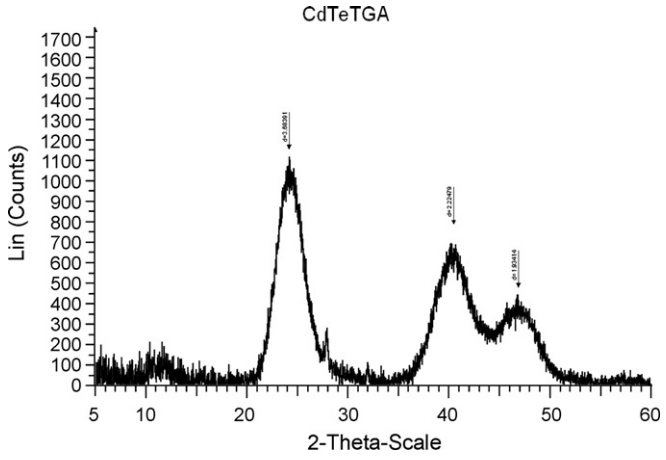

Fig. 3. XRD plot for CdTe–TGA capped QDs.

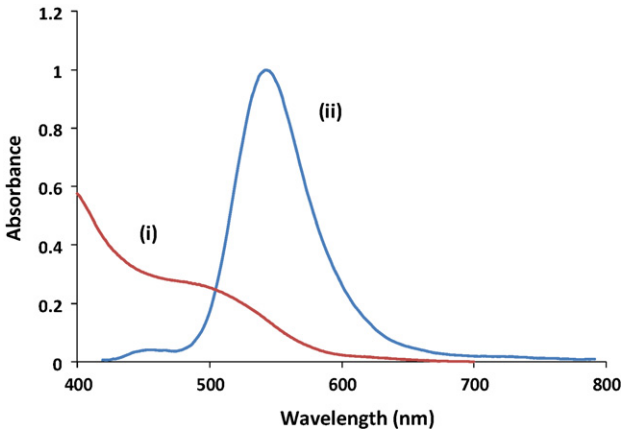

Fig. 4. Absorption (i) and emission (ii) spectra of CdTe QDs (MPA capped) pH 11 buffer. Size of QDs = 2.8 nm. Excitation = 400 nm.

mixed QDs:ZnTAPc (not chemically linked) are eliminated. Ethanol was employed since neither QDs nor ZnTAPc dissolve in this solvent, whereas the QDs were insoluble in THF. The proof for the formation of the amide bond has been provided previously for ZnTAPc–CdTe–MPA, using infrared and Raman spectroscopy [24].

3.2. FRET and fluorescence quenching studies

Förster resonance energy transfer (FRET) is a non-radiative energy transfer from a photoexcited donor fluorophore, after absorption of a higher energy photon, to an acceptor fluorophore of a different species which is in close proximity. The occurrence of FRET is made evident by a decrease of the donor photoemission accompanied by an increase in the acceptor's fluorescence.

For the linked QD–MTAPc complex, excitation was carried out at 550 nm where QDs absorb and MTAPc (in 3:2 DMF:water) does not. No fluorescence was observed for the MTAPc upon excitation at 550 nm. A clear emission peak, however, was observed for ZnTAPc in the QDs:ZnTAPc (linked or mixed), Fig. 6A, upon excitation at this same wavelength, suggesting transfer of energy, through FRET, from the CdTe–TGA QDs to ZnTAPc, as was observed for ZnTAPc–MPA quantum dots, Fig. 6B [24]. Thus this observation of ZnTAPc emission in the presence of QDs, confirms energy transfer from QDs to ZnTAPc. The stimulated emission observed for the linked (QD–ZnTAPc), Fig. 6A, is however, weaker than that for the mixture (QD:ZnTAPc), though the relative amounts of ZnTAPc and

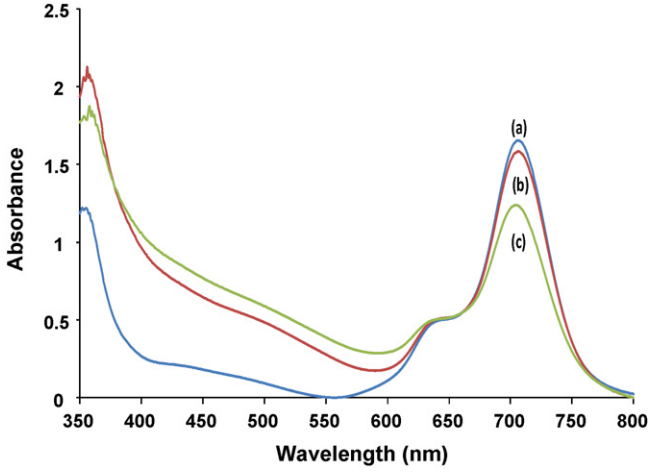

Fig. 5. Electronic absorption spectra of ZnTAPc (a), ZnTAPc + TGA (mixed), (b) and ZnTAPc–TGA (linked) (c) in DMF:water 3:2.

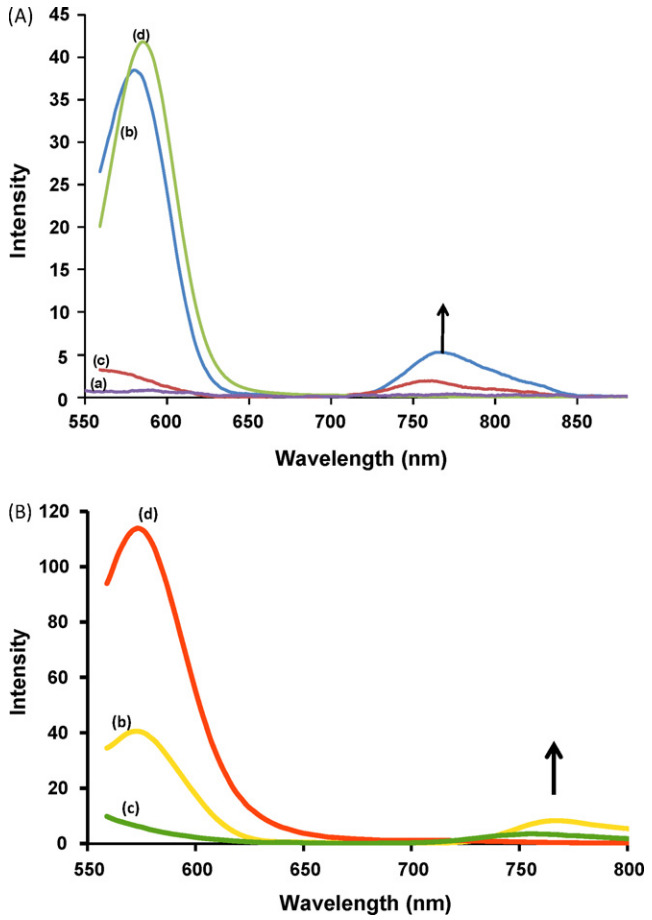

Fig. 6. Emission spectra of (a) ZnTAPc alone, (b) mixed QD–ZnTAPc, (c) linked QD–ZnTAPc and (d) QDs alone. (A) TGA capped QDs and (B) MPA capped QDs. Excitation at 550 nm in DMF:water 3:2. Size = 3.0 nm.

QDs will be different in the mixed and linked QD–ZnTAPc, as was observed for the ZnTAPc–MPA capped QDs [24], making comparison difficult.

No FRET was observed for InTAPc (mixed or linked) in the presence of QDs (MPA or TGA capped), which is probably due to the heavy atom in InTAPc, which results in low fluorescence as most energy in the excited singlet state undergoes intersystem crossing to the triplet state. However, ClInPc was observed to quench the quantum dots' emission, Fig. 7.

The changes in the fluorescence emission spectra of 3.0 nm CdTe–TGA QDs (1.21 mg/ml) in the presence of a range of concentrations (0–7.86×10^{-6} M) of the ZnTAPc are shown in Fig. 7a. These changes are due to the quenching of the fluorescence of the CdTe QDs by the ZnTAPc, due to energy transfer discussed above. The QD's fluorescence was found to decrease progressively with increasing concentration of ZnTAPc. Similar changes were observed for CdTe QDs in the presence of InTAPc, though there was no stimulated Pc fluorescence, Fig. 7b, which is probably due to intersystem crossing of the excited Pc to the triplet state.

Table 1
Quenching and binding constants obtained for MTAPc in the presence of QDs. Size of QDs:CdTe–MPA = 3.5 and 3.0 nm, CdTe–TGA = 3.0 nm. References are in parentheses. Solvent: DMF:water (3:2).

Complex	K (M^{-1})	k_b (M^{-1})	n
ZnTAPc + 3.0 nm MPA	8.08×10^3 [24]	9.55×10^8	2.4
ZnTAPc + 3.0 nm TGA	7.23×10^4	1.26×10^8	1.3
ClInTAPc + 3.0 nm MPA	1.91×10^3	1.06×10^9	1.7
ClInTAPc + 3.0 nm TGA	2.43×10^3	2.76×10^8	1.5
ZnTAPc + 3.5 nm MPA	1.27×10^4	2.98×10^{10}	2.2
ClInTAPc + 3.5 nm MPA	2.92×10^3	4.39×10^9	1.8

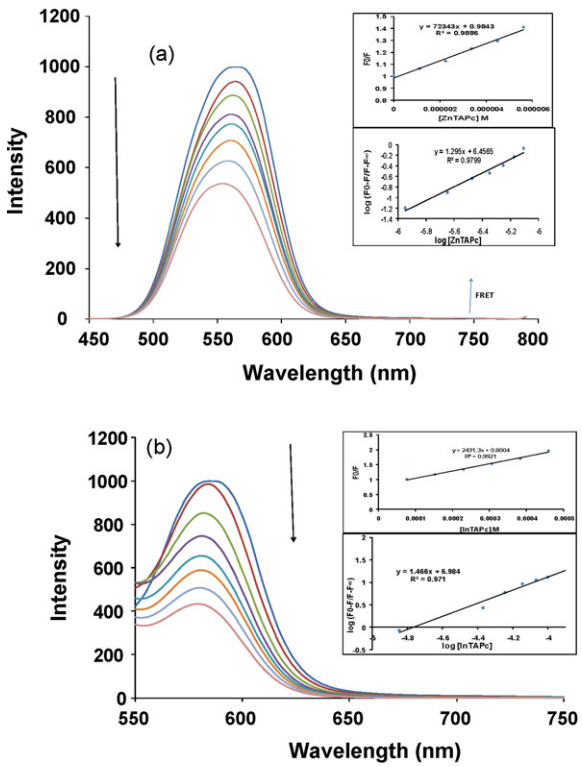

Fig. 7. Variation of the fluorescence spectra of 3.0 nm CdTe–TGA QDs in the presence of varying concentrations of (a) ZnTAPc, [QDs] = 1.21 mg/ml, [ZnTAPc] = 0 to 7.86×10^{-6} M; (b) ClInTAPc, [QDs] = 1.04 mg/ml, [ClInTAPc] = 0–5.37×10^{-4} M. Excitation 550 nm; solvent: DMF:water (3:2).

A plot of F_0/F against [ZnTAPc], Fig. 7a (insert), gives quenching constant (K) values for the quenching of the QDs fluorescence in the presence of ZnTAPc. The linear plot obtained in Fig. 7a (insert) confirmed that the quenching equation (Eq. (5)) was obeyed and a value of 7.23×10^4 M^{-1} was found for K, Table 1. This value (for QDs capped with TGA) is higher than the values reported previously for ZnTAPc ($K = 8.08 \times 10^3$ M^{-1}) in the presence of the same size of QDs capped with MPA [24], Table 1. It is likely that since TGA is a smaller molecule than MPA, there is closer interaction of MTAPc for the former than the latter. K values were also determined for ClInTAPc in the presence of TGA or MPA as capping agents and the data is shown in Table 1 and Fig. 7b. Similarly for ClInTAPc, the K values for ClInTAPc in the presence of TGA capped QDs is larger than that obtained for MPA capped QDs.

K values were generally found to be higher for ZnTAPc when compared to InTAPc (considering the same type and size of QDs),

Table 2
Fluorescence quantum yields of QDs in the absence and presence of MTAPc. Solvent: DMF:water.

QDs[a]	$\Phi_{F(OD)}$	$\Phi^{Mix}_{F(QD)}$	$\Phi^{linked}_{F(QD)}$
CdTe–MPA (3.0 nm)	0.16		
ZnTAPc		0.042	0.011
ClInTAPc		0.051	0.014
CdTe–MPA (3.3 nm)	0.047		
ZnTAPc		0.040	0.017
ClInTAPc		0.014	0.003
CdTe–TGA (3.2 nm)	0.070		
ZnTAPc		0.023	0.021
ClInTAPc		0.019	0.006

[a] Sizes in parentheses and were determined using Eq. (1).

Table 3
Energy transfer parameters for MTAPc in the presence of QDs. Size of QDs: CdTe–MPA = 3.5 and 3.0 nm, CdTe–TGA = 3.0 nm. Solvent: DMF:water (3:2).

MTAPc complex	QDs capping	QDs size (nm)	J (10^{14} cm^6 K)	R_0 (10^{10} m)	r (10^{10} m)	*Eff* (%)
ZnTAPc (mixed) [24]	MPA	3.0	3.43	30.8	25.9	74
ZnTAPc (linked)	MPA	3.0	3.43	30.8	20.0	93
ZnTAPc (mixed)	TGA	3.0	2.18	24.8	22.0	68
ZnTAPc (linked)	TGA	3.0	2.18	24.8	21.6	70
ZnTAPc (mixed)	MPA	3.5	8.90	29.3	39.2	16
ZnTAPc (linked)	MPA	3.5	8.90	29.3	26.6	65
ClInTAPc (mixed)	MPA	3.0	1.02	25.1	22.2	69
ClInTAPc (linked)	MPA	3.0	1.02	25.1	17.0	92
ClInTAPc (linked)	TGA	3.0	0.604	20.0	13.6	91
ClInTAPc (mixed)	MPA	3.5	3.00	24.5	21.2	71
ClInTAPc (linked)	MPA	3.5	3.00	24.5	15.8	93

thus there was less quenching of QDs by the latter. Considering the same type of QDs, but differently sized QDs (e.g. ZnTAPc) mixed with MPA (3.0 and 3.5 nm), the larger QDs were found to bring about larger K values.

The values of the binding constant obtained from the intercepts of the plots of log $\left[\frac{F_0-F}{F-F_\infty}\right]$ vs log [MTAPc] were of the order of 10^8–10^{10} M^{-1}. These values are much higher than those reported for the interaction of CdTe QDs with aluminum tetrasulfonated phthalocyanine (AlTSPc), where the values were of the order of 10^5–10^6 M^{-1} [20]. This could be due to different modes of interaction since AlTSPc is negatively charged while the MTAPc complexes discussed in this work are non-ionic, i.e. the QD capping agent may be repelling the AlTSPc and not the MTAPc. The number of binding sites for MTAPc on QDs were determined (from insets (b) in Fig. 7) to be two (for MPA capped QDs) and one for TGA capped QDs (except a values of close to 1.5 was obtained for InPc–TGA QDs). A value of one has been reported before for AlTSPc and CdTe QDs [20]. The difference could be due to the nature of the MPc molecules.

Fluorescence quantum yields (excitation at 550 nm) of the QDs ($\Phi^{\text{Mix}}_{F(\text{QD})}$) in the mixture with MTAPc decreased slightly, Table 2, compared to $\Phi_{F(\text{QD})}$ of QDs alone, again indicating the quenching of QDs fluorescence by MTAPc. The same applied for the linked MTAPc–QDs.

The efficiency of energy transfer between QDs and MTAPc (*Eff*) was calculated using $\Phi_{F(\text{QD})}$, $\Phi^{\text{Mix}}_{F(\text{QD})}$ and Eq. (7). Since Fig. 5 shows that the absorption spectrum of the QDs in the mixed and linked is about the same, the emission intensity F_{QD} of the QDs in the absence of MPc is assumed to be the same for both the linked and mixed allowing for use of Eq. (4) for determining the $\Phi^{\text{linked}}_{F(\text{QD})}$, and equation (7) for *Eff* for the linked molecule.

Eff is known to be dependent on a number of parameters such as the spectral overlap term (J) estimated by the extent of overlap between the QD emission and the absorbance of the MTAPc derivatives as shown in Fig. 8. In this work the units used for the extent of overlap were cm^6 [32]. The PhotochemCAD program gives J units as cm^6 following the use of $\varepsilon_{\text{MTAPc}}$ in M^{-1} cm^{-1} and the wavelength λ in nm in Eq. (10). The Förster distance, R_0 (Å) is the critical distance between the donor and the acceptor molecule fluorophores for which efficiency of energy transfer is 50% [36,37], and the center-to-center separation distance (r, Å) between donor and acceptor chromophores. The J and R_0 values in this work were computed using PhotochemCAD [35], while the r values were calculated using Eq. (8). All values determined are listed in Table 3.

J values are generally of the order 10^{-14} cm^6 for porphyrin based molecules and the values obtained in this work were found to be in this range, i.e. of the order $\sim 1 \times 10^{-14}$ cm^6 (in general) for the overlap between the QDs and MTAPc, Table 3. As expected, the J values were larger for the larger QDs while r values were found to be smaller than R_0 values indicating that the *Eff* will be greater than 50%, as observed. This applies for all MTAPc–QDs combinations with the exception of ZnTAPc plus MPA (3.5 nm), where r is larger than R_0, and hence *Eff* is less than 50%. The FRET efficiencies reported in this work are higher than reported in the literature [34] for other MPc complexes using the same QDs. For ClInTAPc, FRET was not observed due to the heavy atom effect of In. In all cases, higher *Eff* values were observed for the linked complexes when compared to the mixed QDs–MTAPc combinations, showing the advantages of chemical linking. However, looking at Fig. 6, less QD sensitized MTAPc luminescence was observed for the linked than for mixed, suggesting that even though there is energy transfer from the QDs to MTAPc, not all of the energy is observed as stimulated emission, possibly due to energy losses.

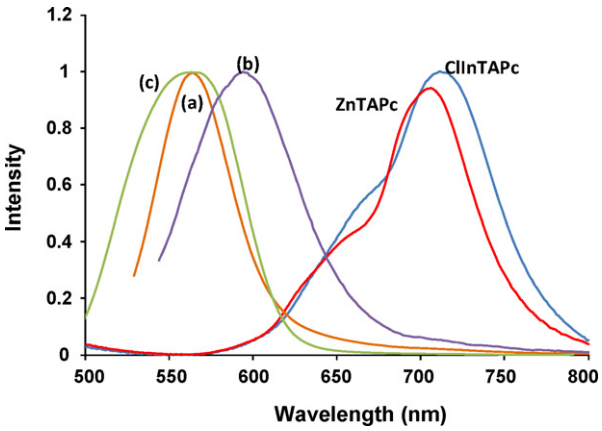

Fig. 8. Absorbance spectra of ZnTAPc and InTAPc in DMF overlayed with the emission spectra of 3.0 nm (a) and 3.5 nm (b) MPA capped CdTe and 3.0 nm TGA (c) capped CdTe in DMF:water 3:2.

The small values of r indicate that the MTAPc is in close proximity to the donor (QD's) and thus there should be an ease of energy transfer (*Eff*) between the excited MPA or TGA capped QD's fluorophore and the MTAPc fluorophore.

4. Conclusion

The results presented give evidence in favour of the formation of an amide bond between MTAPc and CdTe QDs. Both the linked and mixed QDs–ZnTAPc complexes showed Förster resonance energy transfer (FRET), whereas the mixed and linked QD–InTAPc complexes showed no FRET. MTAPc quenched the QDs emission with quenching constants of the order of 10^8–10^{10} M^{-1}. FRET efficiencies larger than 50% were observed, with the linked (MTAPc–QDs) complexes showing better efficiencies than the mixed complexes.

Acknowledgements

This work was supported by the Department of Science and Technology (DST) and National Research Foundation (NRF), South Africa through DST/NRF South African Research Chairs Initiative for

Professor of Medicinal Chemistry and Nanotechnology and Rhodes University. Edith Antunes thanks CSID/Swiss JRF of South Africa for Post-Doctoral funding. Jonathan Britton thanks CSIR South Africa for a graduate bursary.

References

[1] J. Aldana, Y.A. Wang, X. Peng, J. Am. Chem. Soc. 123 (2001) 8844.
[2] J. Guo, W. Yang, C. Wang, J. Phys. Chem. B 109 (2005) 17467.
[3] A.L. Rogach, L. Katsikas, A. Kornowski, D. Su, A. Eychmüller, H. Weller, Ber Bunsenges, Phys. Chem. 100 (1996) 1772.
[4] A.M. Smith, S. Nie, Analyst 129 (2004) 672.
[5] A.C.S. Samia, S. Dayal, C. Burda, Photochem. Photobiol. 82 (2006) 617.
[6] H. Zhang, Z. Zhou, B. Yang, M. Gao, J. Phys. Chem. B 107 (2003) 8.
[7] M.N. Rhyner, A.M. Smith, X. Gao, H. Mao, L. Yang, S. Nie, Nanomedicine 1 (2006) 2091.
[8] A.C.S. Samia, X. Chen, C. Burda, J. Am. Chem. Soc. 125 (2003) 15736.
[9] Z. Liu, C. Liu, Q. Li, Z. Chen, Q. Gong, Rare Metals 25 (2006) 118.
[10] R. Bonnett, Chemical Aspects of Photodynamic Therapy, Gordon and Breach Science, Amsteldijk, The Netherlands, 2000.
[11] I.J. Macdonald, T.J. Dougherty, J. Porphyrins Phthalocyanines 5 (2001) 105.
[12] I. Okura, Photosensitization of Porphyrins and Phthalocyanines, Gordon and Breach Publishers, Amsteldijk, The Netherlands, 2001.
[13] E. Ben-Hur, W.S. Chan, in: K.M. Kadish, K.M. Smith, R. Guilard (Eds.), Porphyrin Handbook, Phthalocyanine Properties and Materials, vol. 19, Academic Press, New York, 2003 (Chapter 117).
[14] I. Rosenthal, Photochem. Photobiol. 53 (1991) 859.
[15] J.D. Spikes, J. Photochem. Photobiol. B: Biol. 6 (1990) 259.
[16] R. Bonnett, Chem. Soc. Rev. 24 (1995) 19.
[17] D. Dini, M. Hanack, in: K.M. Kadish, K.M. Smith, R. Guilard (Eds.), The Porphyrin Handbook, vol. 17, Academic Press, New York, 2003, pp. 23–30 (Chapter 1).
[18] G. de la Torre, C.G. Claessens, T. Torres, Chem. Commun. (2007) 2000.
[19] S. Dayal, R. Krolicki, Y. Lou, X. Qiu, J.C. Berlin, M.E. Kenney, C. Burda, Appl. Phys. B 84 (2006) 309.
[20] M. Idowu, J.Y. Chen, T. Nyokong, New J. Chem. 32 (2008) 290.
[21] J. Ma, J.-Y. Chen, M. Idowu, T. Nyokong, J. Phys. Chem. B 112 (2008) 4465.
[22] S. Dayal, Y. Lou, A.C.S. Samia, J.C. Berlin, M.E. Kenney, C. Burda, J. Am. Chem. Soc. 128 (2006) 13974.
[23] S. Dayal, J. Li, Y.-S. Li, H. Wu, A.C.S. Samia, M.E. Kenney, C. Burda, Photochem. Photobiol. 84 (2007) 243.
[24] J. Britton, E. Antunes, T. Nyokong, Inorg. Chem. Commun. 12 (2009) 828.
[25] L. Jiang, A. Glidle, A. Griffith, C.J. McNeil, J.M. Cooper, Bioelectrochem. Bioenerg. 42 (1997) 15.
[26] B.N. Achar, G.M. Fohlen, J.A. Parker, J. Keshavayya, Polyhedron 6 (1987) 1463.
[27] A. Shavel, N. Gaponik, A. Eychmuller, J. Phys. Chem. B 110 (2006) 19280.
[28] W.W. Yu, L. Qu, W. Guo, X. Peng, Chem. Mater. 15 (2003) 2854.
[29] S. Fery-Forgues, D. Lavabre, J. Chem. Ed. 76 (1999) 1260.
[30] A. Ogunsipe, J.-Y. Chen, T. Nyokong, New J. Chem. 28 (2004) 822.
[31] R.F. Kubin, A.N. Fletcher, J. Lumin. 27 (1982) 455.
[32] J.R. Lakowiecz, Principles of Fluorescence Spectroscopy, 2nd edn., Kluwer Academic/Plenum Publishers, New York, 1999.
[33] J. Rose, Advanced Physico-chemical Experiments, 1st edn., Sir Isaac Pitman and Sons Ltd., London, 1964, pp. 257.
[34] S. Moeno, T. Nyokong, J. Photochem. Photobiol. A: Chem. 201 (2009) 228.
[35] H. Du, R.A. Fuh, J. Li, L.A. Corkan, J.S. Lindsey, Photochem. Photobiol. 68 (1998) 141.
[36] J.S. Hsiao, B.P. Krueger, R.W. Wagner, T.E. Johnson, J.K. Delaney, D.C. Mauzerall, G.R. Fleming, J.S. Lindsey, D.F. Bocian, R.J. Donohoe, J. Am. Chem. Soc. 118 (1996) 11181.
[37] T. Forster, Disc. Far. Soc. 27 (1959) 7.